Analysis of the therapeutic role of stem cells versus selenium nanoparticles in lipopolysaccharide-induced acute lung injury in adult male albino rat: A histological, immunohistochemical and histochemical study

Mohamed Z. Kotb, Doaa A. Abdullah, Mohamed H. Wahdan, Gamal H. Mohamed, Mohammed D.A. Abd Elmoneam

Anatomy and Embryology Department, Faculty of Medicine, Cairo University, Egypt

SUMMARY

Pharmacological research using Lipopolysaccharide (LPS) is a reliable model of acute lung injury. This study aims to compare the therapeutic efficacy of selenium nanoparticles (SeNPs) and bone-marrow-derived mesenchymal stem cells (BMSCs) against lung damage generated by lipopolysaccharides. Fifty adult male albino rats were employed and divided into 5 groups (control group, shame control group, LPS-treated group, SeNPs-treated group, and BMSCs-treated group). Histological and immunohistochemical staining for tumor necrosis factor-alpha (TNFα), Interleukin 6 (IL-6), and Caspase 3 were carried out and followed by histomorphometric analysis. Histochemical measurements of the oxidative-antioxidative markers, superoxide dismutase (SOD), glutathione peroxidase (GPx), and malondialdehyde (MDA) were performed in addition to western blotting analysis to detect the antioxidative activity of Nrf2.

LPS-treated group showed distorted pulmonary architecture with the upsurge in the caspase-3, TNF-α, IL-6, and MDA along with a significant decrease in GPx, SOD, and Nrf2 in the lung homogenates. These findings were relatively improved after adding SeNPs and stem cells. On comparing BMSCs and SeNPs treated group, there was a significant decrease in caspase-3, TNF-α, and IL-6 with BMSCs treatment relative to SeNPs. Treatment with selenium nanoparticles and BMSCs has improved pulmonary changes through their antioxidant and anti-inflammatory role. The level of pulmonary regeneration exerted by BMSCs is better than selenium nanoparticles so the BMSCs may be given preference for a particular course of treatment.

Key words: Lung – Stem cells – Selenium – Lipopolysaccharide – Immunohistochemistry

Corresponding author:
Mohamed Zakaria Kotb. 10 Wali al Ahd Street- Hadayek al Qoba – Cairo.
Phone: +2/01001082011. E-mail: mohamed_zakaria@kasralainy.edu.eg

Submitted: June 23, 2024. **Accepted:** July 18,2024

https://doi.org/10.52083/UNMJ9536

INTRODUCTION

Many bacterial and viral illnesses are known to frequently target the lungs (Gholamnezhad et al., 2022). Acute respiratory distress syndrome (ARDS) is a common consequence of acute lung injury (ALI) with limited effective therapeutic options (Tian et al., 2022).

Lipopolysaccharide (LPS) is a popular pathogenic endotoxin utilized to create ALI pharmacological research models. In LPS-induced ALI, there is an increase in reactive oxygen species (ROS) generated by neutrophils and activated macrophages sequestered in the pulmonary vasculature (Mokhtari-Zaer et al., 2020; Peng et al., 2022).

Vijayakumar et al. (2022) observed that selenium has a key function in balancing the redox system and proper functioning of the immune system. Selenium nanoparticles (SeNPs) attracted a lot of attention because of their novel characteristics such as high surface area and lower risk of selenium toxicity. SeNPs have been shown in numerous studies to exhibit anti-inflammatory properties, anticancer effects, and a potential preventive agent both in vivo and in vitro and anticancer effects.

Mesenchymal stem cells (MSCs) are extracted from adult organs such as bone marrow, fat, and umbilical cord blood. They can preserve and regenerate mesenchymal tissues through differentiation into many lineages, such as adipose tissue, bone, cartilage, and muscle (Gebraad et al., 2022).

The present study was assigned to study the histological, immune-histochemical, and histochemical adverse changes of the lung of adult albino rats following lipopolysaccharide- induced lung injury and to evaluate the therapeutic efficacy of stem cells versus nano-selenium against such changes.

MATERIALS AND METHODS

Animals

Fifty adult male Sprague-Dawley albino rats weighing 180-220 g were used in this study. Before administering the medication, the rats were given two weeks to get used to the lab environment. Each of the five rats was kept in a separate cage. The Animal and Experimental House, Cairo University's Faculty of Medicine, was the site of the experiment. The animals were treated following the standards that Cairo University's Institutional Animal Care and Use Committee (IACUC) approved under protocol number CU III F 52 20. Throughout the trial, the animals had unlimited access to water and a standardized laboratory meal.

Chemicals

Lipopolysaccharides (LPS): 100 ml solution was obtained from Sigma-Aldrich Chemical Co. Egypt. It was given as a single dose of 0.5 mg /kg by IP injection (Dos Santos Haupenthal et al., 2020), Selenium nanoparticles (SeNPs): were purchased from Nanotech. Egypt as a powder of 100 g dissolved in 100 ml ethanol solution. It was administered at a dose of 0.5 mg/kg daily for five consecutive days by IP injection (Shahabi et al., 2021), and Fluorescent labeled BMSCs: were obtained from the Biochemistry Department, Faculty of Medicine Cairo University at a concentration of $1x10^6$ unit /ml. It was given as a single dose of (1×10^7) BMSCs diluted in 200 **µL** PBS by injection into the tail vein (Feng et al., 2019).

Isolation, culture, and labeling of BMSCs

To separate BMSCs, xylazine and ketamine injections intraperitoneally were used to anesthetize the hamsters. They were trypsinized twice to extract a sufficient number of cells (Zhang et al., 2014). Red fluorochrome PKH26 was used to label undifferentiated MSCs following manufacturer instructions (Sigma, Saint Louis, Missouri, USA). The labeled cells appeared as red spots under an x100 magnification fluorescence microscope (Leica-Germany).

Experimental design

The rats were randomly allocated into 5 groups (10 rats each), *Group I* (normal Control): which received nothing, then the rats were sacrificed on the 7th day of the experiment, *Group II* (sham control) which were further subdivided into two subgroups, Subgroup a: 5 rats which received a single dose of 0.5 ml/kg normal saline (solvent of LPS)

by intraperitoneal (IP) injection, the rats were sacrificed on the 7th day of the experiment, and Subgroup b: 5 rats which received a single dose of 0.5ml/kg normal saline by IP injection.

Twenty-four hours later the rats were given ethanol at a daily dose of 0.5 ml/kg (solvent of nanoselenium) for 5 consecutive days by IP injection, the rats were sacrificed on the 7th day of the experiment, *Group III* (LPS treated group) which received LPS as a single dose of 0.5 mg /kg by IP injection on the first day of the experiment (Dos Santos Haupenthal et al., 2020), the rats were sacrificed on the 7th day of the experiment, *Group IV* (LPS & SeNPs treated group) which were given LPS as a single dose of 0.5 mg /kg by IP injection on the first day of the experiment. Twenty-four hours later the rats were given selenium nanoemulsion at a daily dose of 0.5 mg/kg for five consecutive days by IP injection (Shahabi et al., 2021); the rats were sacrificed on the 7th day of the experiment. *Group V* (LPS & Stem cell treated group), which were given LPS as a single dose of 0.5 mg/kg by IP injection on the first day. Twenty-four hours later the rats were given a single dose of (1×10^7) BMSCs diluted in 200 µL PBS by injection into the tail vein (Feng et al., 2019); the rats were sacrificed on the 7th day of the experiment.

At the end of the experiment (24 hours after the last dose of Selenium nanoparticles), the rats of each group were anesthetized by intraperitoneal injection of phenobarbital sodium 40 mg/kg (Laferriere and Pang, 2020). Then the rats were sacrificed by cervical dislocation and the lung was excised and dissected. Fresh lung specimens were taken for histochemical study to measure the oxidative markers in the lung homogenates. The remaining portion was fixed in 10% buffered formol saline and ready for paraffin block preparation. Five µm thick semi-serial sections were cut and subjected to:

Light microscopic study

Lung sections of each rat were stained with Hematoxylin and Eosin stain for routine histological examination, and unstained sections were used to detect fluorescent labeled BMSCs under the fluorescent microscope.

Immunohistochemical study

Anti-tumor necrosis factor-alpha and anti-Interleukin 6 antibodies were used (Sigma- Aldrich chemical company, Egypt at a dilution 1:100) to detect the pro-inflammatory cytokines, tumor necrosis factor-alpha (TNFα) and interleukin 6 (IL6) (García-García et al., 2022). Anti-caspase 3 rabbit monoclonal antibody was also used (Abcam Company, Cairo, Egypt, Catalog, ab184787 at a dilution 1:1000) to detect the apoptosis marker, caspase-3 (Ayoub and El Beshbieshy, 2016).

Histochemical study

Superoxide dismutase (SOD) and Glutathione peroxidase (GPx) activities in lung tissue homogenate were measured as an oxidative marker by the inhibition of nitroblue tetrazolium reduction by O_2-generated by the xanthine/xanthine oxidase system (Arab Sadeghabadi, et al., 2019) by the method of Lowry et al. (1951) using BSA as a standard. Malondialdehyde (MDA) level in lung tissue homogenate was measured as an index of lipid peroxidation in tissues. Its level was estimated with the Thiobarbituric acid (TBA) method (De Leon and Borges, 2020).

Western Blotting analysis: to detect the antioxidative activity of Nrf2, the total protein of lung tissues and cells was extracted, and the protein concentrations were determined using the BCA Protein Assay Kit (Beyotime, China) (Yang, et al., 2019).

Morphometric measurements

Quantitative study was obtained with the aid of J image analysis (IMD, USA) and Lica Qwin 500 LTD (England) using the software Quin 500 (England). The study involved assessment of thickness of inter-alveolar septa in (µm) and the area percent of immunohistochemically positive structures in TNFα, IL6, and caspase 3 immunohistochemically stained sections.

Statistical analysis

SPSS version 21.0 (IBM Corporation, Somers, NY, USA) was employed for the statistical analysis. The information was presented as means ± standard deviation. ANOVA testing and Bonferroni

pairwise comparisons were used for statistical evaluation. P values less than 0.05, were regarded as significant; when they were less than 0.001, they were considered extremely significant (Armitage et al., 2008).

RESULTS

There was no mortality noticed in the rats of the four groups of the experiment.

Histological results (Fig. 1)

H&E-stained lung sections of groups I and II revealed normal spongy pulmonary architecture consisting of several variable-sized patent alveoli and alveolar sacs separated by thin interalveolar septa. The alveoli were lined by two types of pneumocytes: flat squamous epithelial cells with flattened nuclei (pneumocyte Type I) and large cuboidal cells with rounded nuclei (pneumocyte Type II). Thin-walled respiratory bronchioles and small branches of the pulmonary arterioles were seen among the alveoli within the pulmonary parenchyma.

The LPS-treated group's lung sections displayed severely deformed pulmonary architecture, including collapsed alveoli and noticeably thicker inter-alveolar septa packed with extravasated red blood cells and mononuclear inflammatory cells. Large irregular emphysematous air gaps and dilated alveoli with ruptured interalveolar septa were observed in certain regions. Some specimens had extensive alveolar and interstitial hemorrhage. Many detached alveolar epithelial cells were observed in the alveolar lumen. Massive peri-bronchial cellular infiltration and extensive exfoliation of the lining epithelial cells were indicative of bronchiolar affection. Additionally, there was a noticeable interstitial eosinophilic exudate and vascular congestion.

Sections of the lungs of the SeNPs-treated group showed marked improvement in the pulmonary

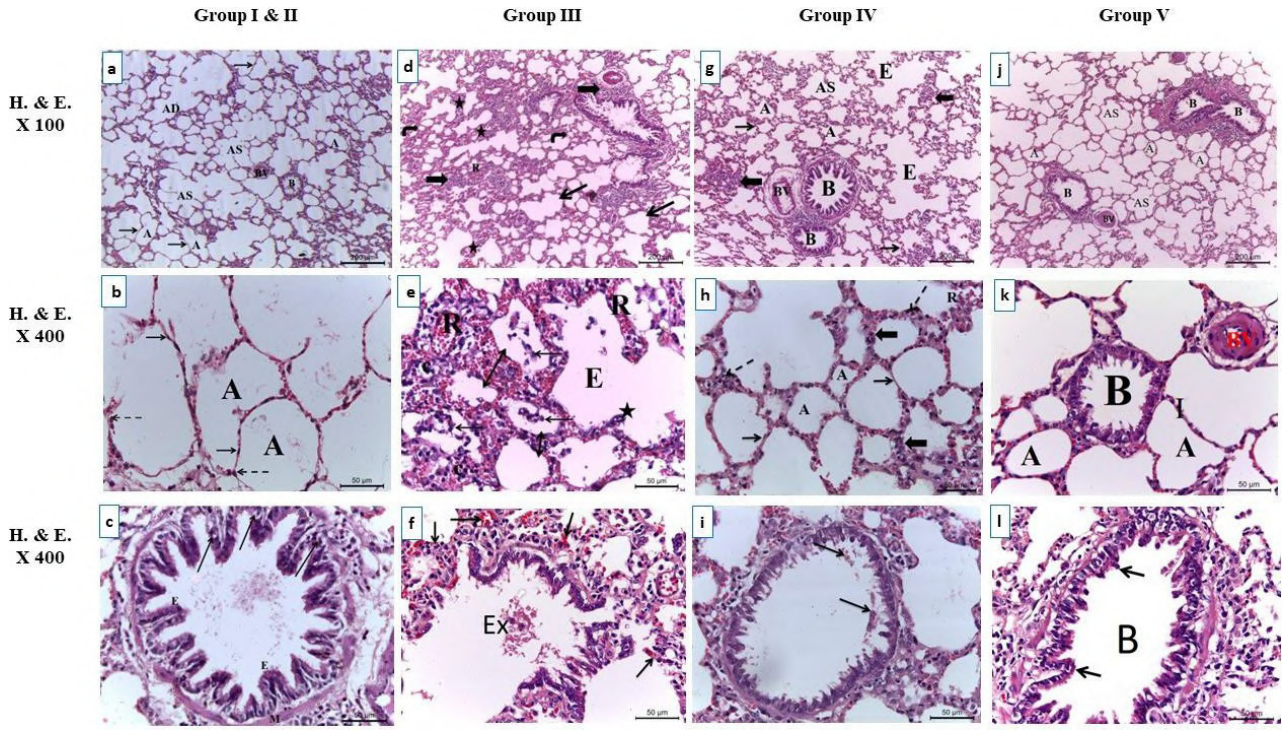

Fig. 1.- Lung sections of different groups. Groups I & II: **(a)** showed normal pulmonary architecture consisting of alveolar sacs (AS), alveolar ducts (AD), alveoli (A), thin inter-alveolar septa (arrow). Thin-walled blood vessels (BV) and respiratory bronchiole (B). **(b)** alveolar lining consisting of pneumocytes type I with flat nucleus (arrow) and pneumocytes type II with rounded nucleus (dashed arrow). **(c)** bronchioles lining formed of simple columnar epithelial cells (E) with goblet cells (arrow) and surrounded by smooth muscle layer (M). Group III: **(d)** distorted pulmonary architecture in the form of collapsed alveoli (curved arrow), dilated alveoli (straight arrow), thick inter-alveolar septa (stars) studded with extravasated RBCs (R) and mononuclear inflammatory cells (thick arrow). **(e)** area of ruptured interalveolar septa (star) with large irregular emphysematous air space (E). Detached alveolar epithelial cells in the alveolar lumen (arrows). **(f)** massive peri-bronchial cellular infiltration and extravasated RBCs (arrows) with exfoliation of the bronchial epithelial cells lining (Ex). Group IV: **(g, h)** partial improvement of pulmonary architecture apart from few thickened inter-alveolar septa (thick arrow) with minimal mononuclear cellular infiltration and extravasated RBCs (R). Few areas of ruptured inter-alveolar septa with large emphysematous air spaces (E). **(i)** showed minimal sloughing of the bronchial epithelium (arrows). Group V **(j, k, l)** showed nearly complete restoration of the normal pulmonary tissue. Scale bars: a, d, g, j = 200 µm; b, c, e, f, h, I, k, l = 50 µm.

architecture. The lung parenchyma was nearly recovered: apart from mild inflammatory infiltrate aggregates, few areas of ruptured interalveolar septa with large irregular emphysematous air spaces, some interalveolar septa are still thickened with minimal mononuclear cellular infiltration, and extravasated RBCs and minimal sloughing of bronchial epithelium.

The lungs of rats treated with stem cells displayed improvement in the bronchial and arteriolar architecture.

Immunohistochemical results (Fig. 2)

Caspase-3: The control group showed negative caspase-3 immuno-expression. Meanwhile, the LPS-treated group revealed strong positive caspase-3 immuno-reactivity. On the other hand, a marked reduction of apoptotic cells with moderate caspase-3 positive cells was observed with SeNPs treatment. Few positive caspase-3 immunostaining was noticed with stem cell treatment.

TNF-α: Immunoreaction to TNF-α showed minimal expression in the cytoplasm of alveolar pneumocytes type I and type II of the control and sham control groups. There were strongly positive TNF-α immunostaining cells detected in the alveolar cells of the LPS group. Mild active TNF-α immunostaining cells were seen in the pneumocytes of the SeNPs-treated group. The positive TNF-α immunostaining cells were limited in the stem cells treated group.

Interleukin -6: Immunoreaction to IL-6 was negative in the control and sham groups. While the LPS-treated group showed an intense IL-6-expressed reaction. On the other hand, the positive IL-6 immunostaining cells were moderate in sections of the SeNPs-treated group, and nearly negative in the stem cells-treated group.

Histochemical results

MDA: a statistically significant rise in the MDA level was seen in the lung homogenates of the LPS group. By contrast, treatment with SeNPs in group IV and BMSC in group V showed a statistically non-significant rise in comparison to the control and sham groups. The difference in MDA level between groups IV and V was statistically not significant (Bar chart 1).

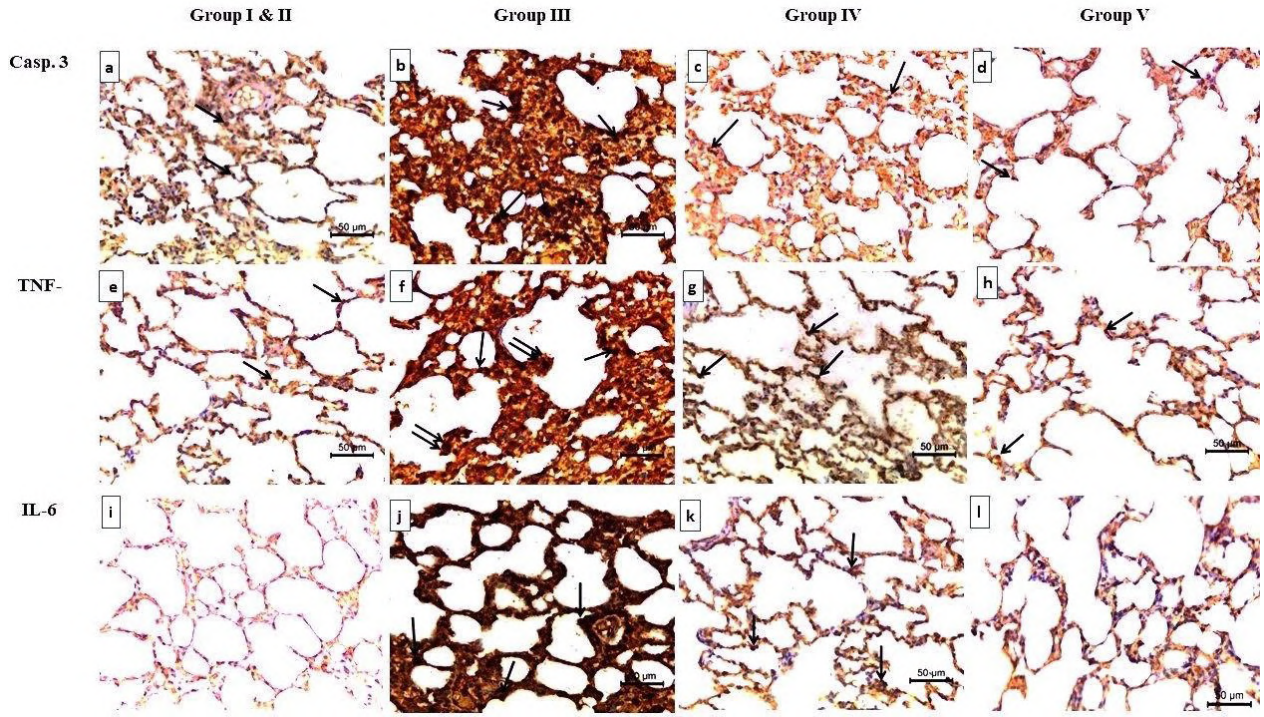

Fig. 2.- Photomicrograph of different lung sections stained by anti-caspase-3, anti TNF-α and anti-IL-6 showing various cytoplasmic reaction, Both control and stem cells treated groups showed minimal positive anti caspase reaction **(a, d)**, anti TNF-α reaction **(e, h)** and anti-IL-6 reaction **(i, l)**. LPS group showed marked positive anti caspase reaction (b), anti TNF-α reaction **(f)** and anti-IL-6 reaction **(j)**. **(c)** Selenium treated group showed moderate positive anti caspase reaction (c), anti TNF-α reaction **(g)** and anti-IL-6 reaction **(k)**. Scale bars = 50 µm.

SOD: SOD activity showed a highly significant decrease in the LPS-treated group. Treatment with SeNPs in group IV and BMSC in group V showed a non-significant decline relative to the control and sham groups. While comparing the same values between group IV and group V revealed a statistically non-significant difference (Bar chart 2).

GPx: GPx activity showed a highly significant decrease in the LPS-treated group. Treatment with SeNPs in group IV and BMSC in group V showed a non-significant decline relative to the control and sham groups. While comparing the same values between group IV and group V revealed a statistically non-significant difference (Bar chart 3).

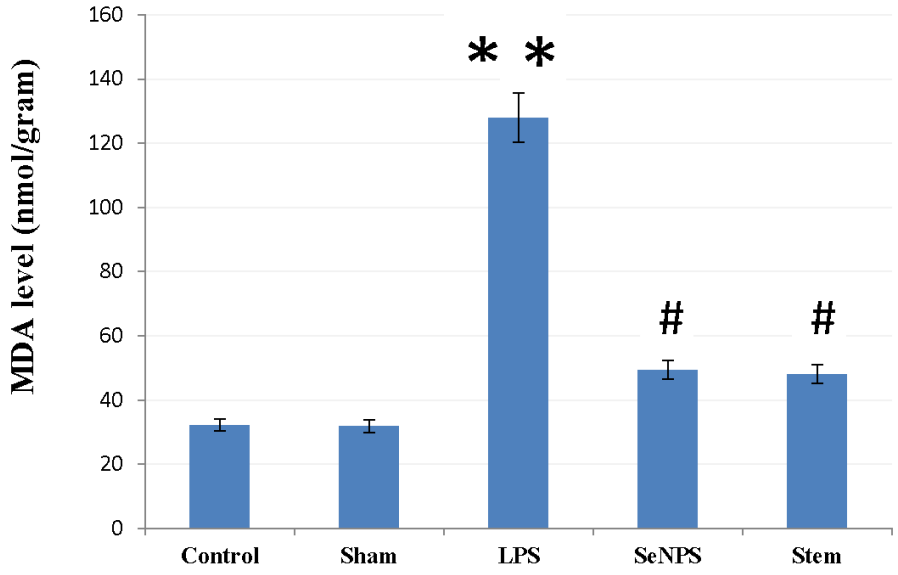

Bar chart 1. Mean area % ± SD of MDA level in the different experimental groups. Using ANOVA followed by Bonferroni pairwise comparisons, **: Statistically highly significant P value ≤ 0.001 compared to control group. #: highly significant compared to LPS group.

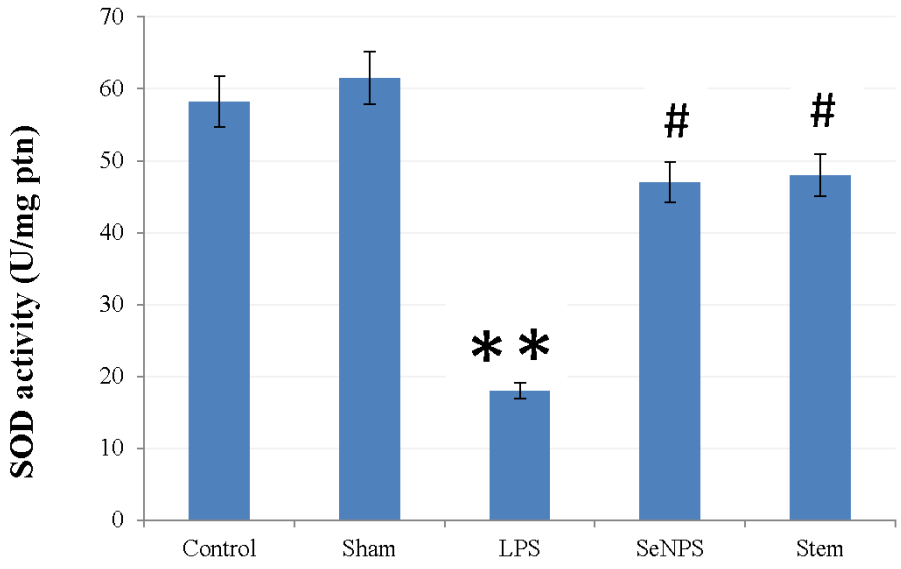

Bar chart 2. Mean area % ± SD of SOD activity in the different experimental groups. ** Statistically highly significant P value ≤ 0.001 compared to control group. #: highly significant compared to LPS group.

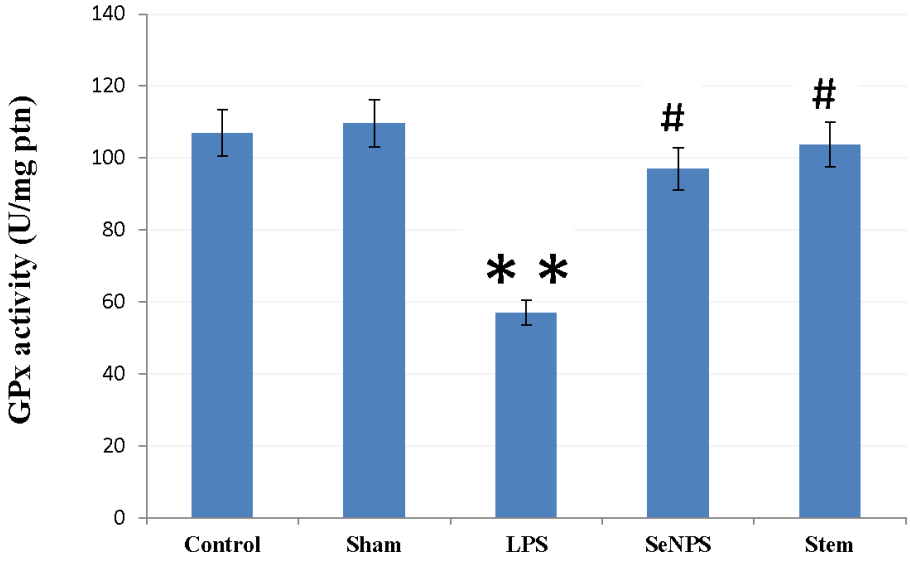

Bar chart 3. Mean area % ± SD of GPx activity in the different experimental groups. ** Statistically highly significant P value ≤ 0.001 compared to control group. #: highly significant compared to LPS group.

Western blot assay: Assessment of the relative expression of Nrf2 showed a highly significant decrease in the LPS-treated group relative to the control and sham groups. Treatment with SeNPs in group IV and BMSC in group V showed a non-significant decline relative to the control and sham groups. Comparing the same values between group IV and group V revealed a statistically significant increase in the relative expression of Nrf2 in group V (Bar chart 4).

Morphometric results

Thickness of interalveolar septa in the lung tissue: Thickness of interalveolar septa revealed a highly significant increase in the LPS-treated group. Treatment with SeNPs in group IV and BMSC in group V revealed a statistically non-significant increase relative to the control and sham groups. Comparing the same values between group IV and group V revealed a non-significant difference (Bar chart 5).

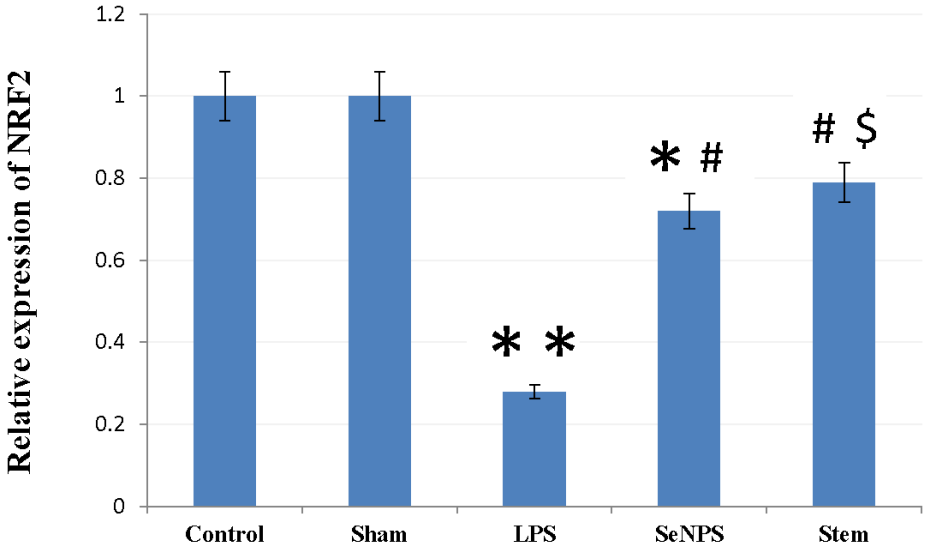

Bar chart 4. Mean area % ± SD of relative expression of Nrf2 in the different experimental group. *: Statistically significant P value ≤ 0.05 compared to control group. ** Statistically highly significant P value ≤ 0.001 compared to control group. #: highly significant compared to LPS group. $: Statistically significant compared to SeNPs group

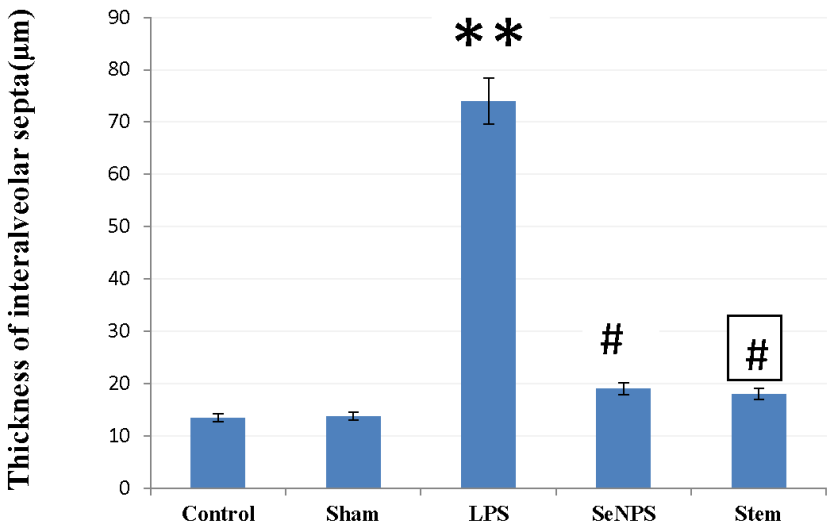

Bar chart 5. Mean area % ± SD of thickness of interalveolar septa in the different experimental groups. ** Statistically highly significant P value ≤ 0.001 compared to control group. #: highly significant compared to LPS group

Area percentage of caspase 3 immuno-reactivity: The histomorphometric study of caspase 3 immuno-expression revealed a highly statistically significant increase in the LPS-treated group relative to the control and sham groups. On the other hand, treatment with SeNPs in group IV and BMSC in group V revealed a statistically non-significant increase. Comparing the same values in groups IV and V revealed a statistically significant decrease in the mean area of caspase 3 in group V (Bar chart 6).

Area percentage of TNF-α immune expression: The histomorphometric study of TNF-α immune expression revealed a highly significant increase in the LPS group. Treatment with SeNPs in group IV and BMSC in group V revealed a non-significant increase relative to the control and sham groups. At the same time, comparing the same values between group IV and group V revealed a statistically significant decrease in group V relative to group IV (Bar chart 7).

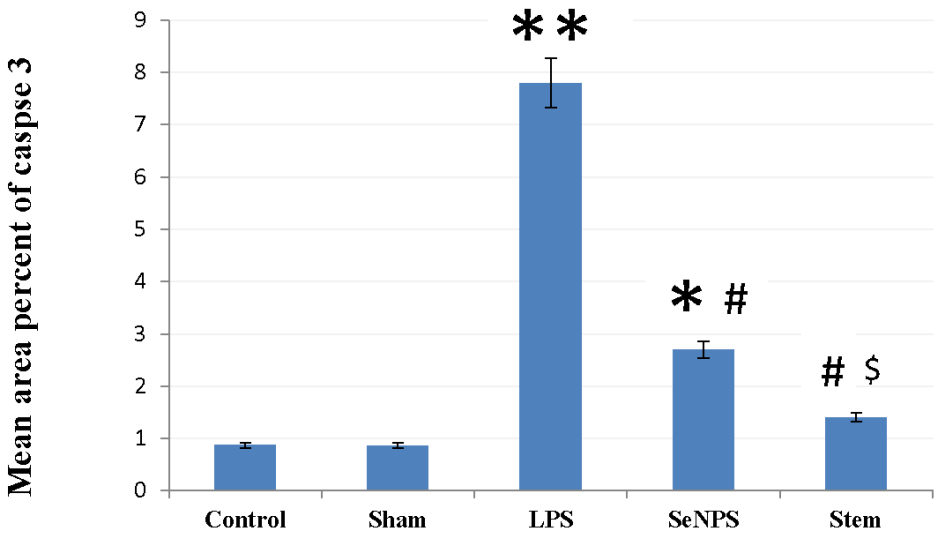

Bar chart 6. Mean area % ± SD of caspase 3 immunoexpression of in the different experimental groups. *: Statistically significant P value ≤ 0.05 compared to control group. ** Statistically highly significant P value ≤ 0.001 compared to control group. #: highly significant compared to LPS group. $: Statistically significant compared to SeNPs group.

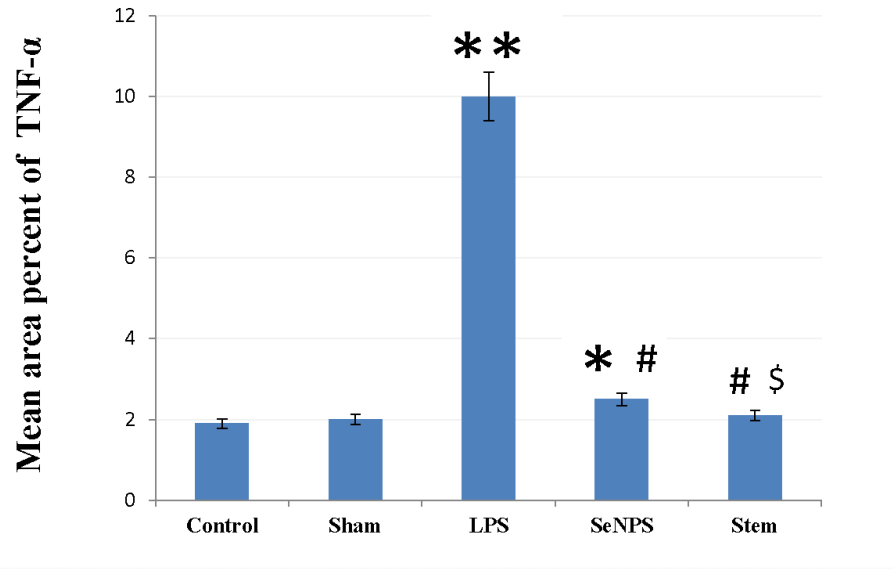

Bar chart 7. Mean area % ± SD of TNFα immunoexpression in the different experimental groups. *: Statistically significant P value ≤ 0.05 compared to control group. ** Statistically highly significant P value ≤ 0.001 compared to control group. #: highly significant compared to LPS group. $: Statistically significant compared to SeNPs group

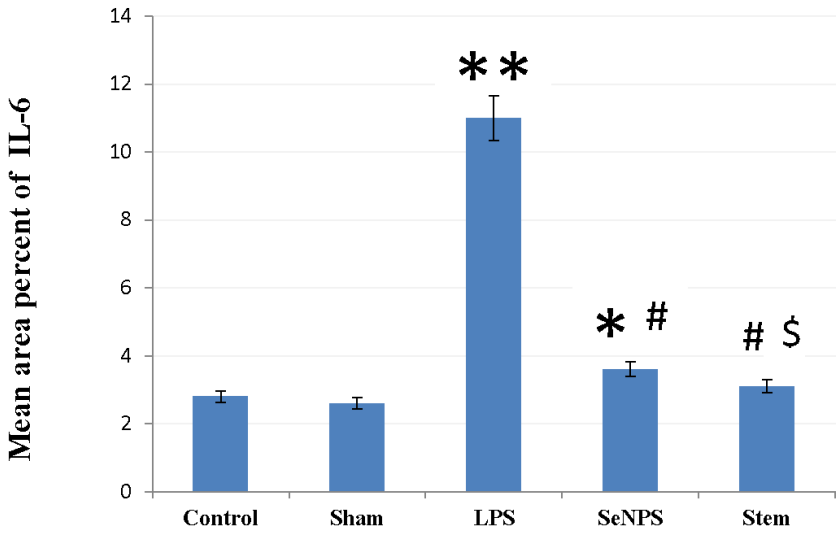

Bar chart 8. Mean area % ± SD of IL6 immunoexpression in the different experimental groups. *: Statistically significant P value ≤ 0.05 compared to control group. ** Statistically highly significant P value ≤ 0.001 compared to control group. #: highly significant compared to LPS group. $: Statistically significant compared to SeNPs group

Area percentage of IL-6 immuno-expression: The histomorphometric study of IL-6 immuno-expression revealed a highly significant increase in the LPS group. Treatment with SeNPs in group IV and BMSC in group V revealed a statistically non-significant increase relative to the control and sham groups. At the same time, comparing the same values between group IV and group V revealed a statistically significant decrease in group V relative to group IV (Bar chart 8).

DISCUSSION

This study investigated the effects of BMSC therapy versus SeNP administration on lipopolysaccharides-induced lung injury.

In this study, the administration of lipopolysaccharides (LPS) resulted in numerous pathological changes in the lung's histological architecture, which manifested as focal areas of collapsed alveoli, damaged alveoli, and a noticeable thickening of the interalveolar septa that were invaded by inflammatory cellular aggregates. Our finding was established by Zhang et al. (2018) and Wu et al. (2019), who found serious pulmonary lesions such as thickening of the alveolar wall and extensive inflammation after LPS administration. This comes in agreement with Domscheit et al. (2020), who attributed those LPS-induced changes to the lung's production of cytokines, which causes neutrophil infiltration and lung damage.

This work revealed fluid exudates between some alveoli and around blood vessels in group III. These results were matched with Badamjav et al. (2020), who suggested these histopathological changes to troubles in vascular permeability brought on by the LPS toxicity. In this research, sporadic areas in the lung of group III revealed increased goblet cells in the bronchi. Some writers have suggested that bronchial inflammation can cause augmented mucus secretion as a result of chronic bronchitis and lung parenchyma loss, which can lead to emphysema (Raafat et al., 2018). Mononuclear cellular infiltration was another histological finding in the LPS-treated group. This comes in agreement with Mokhber Dezfouli et al. (2018), who found inflammation and lymphocytic infiltration in lung tissues treated with LPS. The same authors attributed these findings to oxidative damage and ROS; superoxide anion and hydroxyl radicles induced by LPS.

This immunohistochemical study revealed a highly significant increment in the area percent of caspase3 reaction in the lung tissue of group III (LPS-treated) rats. This result matches that obtained by Ye et al. (2020), who suggested that ROS induced by LPS causes an inflammatory response with many macrophages, inhibition of mitochondrial function, and results in DNA damage and apoptosis.

As regards pro-inflammatory cytokines in the lung, the present work revealed a highly significant increase in TNF-α and IL-6 immune reactions. The existing study illustrated that MDA level (the lipid peroxidation end product), was significantly increased in group III (LPS- treated group). These findings come in parallel to the results of Soliman et al. (2018) and Liu et al. (2022), who mentioned that pulmonary MDA displayed a significant increment in the LPS- injected group. The last authors explained that the increase in MDA could be attributed to the depletion of the antioxidant system. Our results come with a reduction in SOD activity in the lungs in the LPS group. This may be explained by the significant inflow of superoxide radicals, which in turn produce a lot of H2O2 and subsequently impede SOD activity. This finding comes in agreement with Sha et al. (2019), who reported a significant decrease in SOD activity of the liver treated with LPS.

Morphometrically, the LPS group's interalveolar septa showed a statistically significant increase in thickness. This finding is coinciding with that of dos Santos Haupenthal et al. (2020), who stated that, after intraperitoneal administration of LPS, there was an increment in the alveolar wall thickness. This observation may be explained by a notable cellular infiltration, particularly in the perivascular and peribronchiolar regions, where there is increased collagen deposition, signifying fibrosis. Our results revealed a decrement in the relative expression of Nrf2 in the lung homogenates of the LPS-treated group. Zhang et al. (2018) and Yang et al. (2019) reported comparable results in mouse and duck lung tissues, respectively. Sun et al. (2021) also reported the involvement of the Nrf2-ARE pathway in acute and chronic lung injury. Similarly, Liu et al. (2022) observed that LPS decreased the Nrf2-ARE signaling

The histological findings of the current study illustrated that SeNPs treated rats (group IV) revealed marked improvement of the pulmonary architecture, nearly normal lung parenchyma together with few still degenerated emphysematous areas. Some inflammatory infiltrate and minimal extravasated RBCs were still present. This is concordant with Shahabi et al. (2021), who postulated that by lowering the levels of TNF-a and TGF-b, SeNPs can release inflammation. Also, the last authors found that nanoparticles' ability to withstand enzymatic breakdown is linked to increased bioavailability and decreased

drug clearance. Furthermore, sustained release profiles and decreased toxicity are linked to nano-sized drug delivery systems. In this research, a marked reduction of apoptotic cells with moderate caspase-3 positive cells was observed in SeNPs-treated rats (group IV). Al-Kahtani and Morsy (2019) found that SeNPs could induce the anti-apoptotic protein Bcl-2 level in the liver tissue of the Aluminum Chloride-SeNPs rat group. Regarding the inflammatory markers, the immuno-histological and immunohistochemical study of group IV revealed that the positive TNF-α immuno-stained cells showed a highly statistically significant decrease relative to the LPS-treated group. This is consistent with earlier research of Zaafan et al. (2016) and El-Ghazaly et al. (2017), who showed that SeNPs have anti-inflammatory properties and were able to dramatically lower the level of TNF-a and relieve radiation-induced inflammatory response in experimental animals. Additionally, our findings were also established by a recent study conducted by Gad et al. (2021), and demonstrated a significant reduction in the inflammatory markers TNF-α, TGF, IL-6, and IL-2 in the SeNP- treated HepG2 cell lines. The histological outcomes of this study exhibited that stem cells treated rats (group V) revealed an improved histological picture. This matches the results of Soliman et al. (2018), who indicated that BMMSCs resulted in normal morphology of lung tissue via higher antioxidant enzyme activities and lower MDA levels and myeloperoxidase (MPO) activity in the MSC recipient groups.

The histomorphometric study of the thickness of interalveolar septa revealed a statistically significant decrease in both SeNPs and stem cells treated groups. Moreover, the stem cell group revealed a noticeable diminution compared to the SeNPs-treated group.

This comes in agreement with those of Shalaby et al. (2014) and Zakaria et al. (2021) who attributed this finding to the anti-inflammatory effect of MSCs. Our results proved that stem cells migrated from the bloodstream to the lungs in the stem cell-treated group by fluorescent microscopic examination of the lung tissue and interalveolar spaces. Barry and Murphy (2004) stated that the exact process through which MSCs were guided to the tissues and moved across the endothelium is still unknown. However, it is more likely that the injured tissue expresses specific ligands or receptors and releases a variety of chemotactic factors. The released factors facilitate traffic, adhesion, and infiltration of MSCs to the site of injury. Lu et al. (2017) mentioned that the improvement induced by BMSCs, on acute necrotizing pancreatitis, was due to their regenerative effect on the injured capillary endothelial cells and the increased expression of aquaporin 1. Wu and Tang (2021) and Flores et al. (2022) added that MSCs, in rats, secrete molecules that have local and distal anti-inflammatory effects.

The present study showed very few active caspase-3 immunostaining cells in the stem-cells-treated group, which indicate a marked reduction of apoptosis. Along the same line, El Bana and Shawky (2019) also reported a significant decline in the collagen fibers and caspase-3 expression in rats treated with stem cells after amiodarone lung toxicity. Decreased apoptosis in response to mesenchymal stem cell therapy has been reported by Li et al. (2016), Zhang and Shi (2017), and Song et al. (2017) in rat muscles, Schwann cells, and myocardium, respectively.

The decreasing effect of BMSCs on MDA levels in the current study is consistent with the findings of Hu et al. (2021), who confirmed the ability of MSCs in tissue regeneration.

Regarding the oxidative/anti-oxidative stress markers in the present study, both SOD and GPx were significantly amplified in both SeNPs and stem cells treated groups. Furthermore, stem cell groups elucidated a significant increase in their levels than the SeNPs-treated group. The augmenting role of BMSCs on the SOD level, in this study, is in agreement with the results of Soliman et al. (2018) and Wu et al. (2022). The increasing effect of BMSCs, on GPx level also runs by the results of Maltaib et al. (2017) and Zhang and Shi (2017); all of these authors related this effect to the release of soluble growth factors from MSCs. AlKahtani and Morsy (2019) added that antioxidant indicators were found to be greatly replenished by SeNPs administered to rats injected with aluminum, approaching normal values. Since GPx is an enzyme

that depends on selenium (SeNPs), adding SeNPs to a supplement may increase the enzyme's activity and content, which would then reverse oxidative damage. Sentkowska and Pyrzyńska (2022) explained that SeNPs' wide surface area and smaller size allow them to be exposed to more free radicals for electron exchange, which gives them strong antioxidant properties. As a result, SeNPs show strong scavenging activity against a variety of free radicals. In our study, assessment of Nrf2 of the SeNPs and stem cell groups revealed a significant upsurge. This comes in agreement with Ni et al. (2015), who proved that Nrf2 activation served as the primary protective mechanism of nanoselenium particles. Song et al. (2017) stated BMSCs, as an activator of Nrf2, have a potent antioxidative effect. Nrf2 separates from KEAP-1 in response to the stimuli and attaches itself to ARE in the nuclear membrane. Antioxidative gene expression may then be encouraged as a result. Consequently, the biological impact of BMSCs may be pertinent to the removal of ROS via Nrf2 signaling. Another confirmatory result was reported by Wang et al. (2022), who showed that the treatment of BNS increased the expression of Nrf2 and the genes that are downstream of it. This suggests that the Keap1-Nrf2-ARE pathway is activated by nanoselenium to reduce oxidative stress, inflammation, cytotoxicity, and maybe genotoxicity.

The current study's findings supported earlier research's descriptions of SeNPs' potential benefits against oxidative stress and their ability to prevent the generation of free radicals (Song et al., 2017; Gad et al., 2021).

Our study concluded that treatment with selenium nanoparticles and BMSCs has triggered significant improvement in the histological and biochemical pulmonary changes. The extent of pulmonary regeneration exerted by BMSCs is better than selenium nanoparticles.

REFERENCES

AL-KAHTANI M, MORSY K (2019) Ameliorative effect of selenium nanoparticles against aluminum chloride-induced hepatorenal toxicity in rats. *Environ Sci Pollut Res*, 26(31): 32189-32197.

ARAB SADEGHABADI Z, ABBASALIPOURKABIR R, MOHSENI R, ZIAMAJIDI N (2019) Investigation of oxidative stress markers and antioxidant enzymes activity in newly diagnosed type 2 diabetes patients and healthy subjects, association with IL-6 level. *J Diabetes Metab Disord*, 18: 437-443.

ARMITAGE P, BERRY G, MATTHEWS JNS (2008) Statistical methods in medical research. John Wiley & Sons.

AYUOB N, ELBESHBEISHY R (2016) Impact of an energy drink on the structure of stomach and pancreas of albino rat: can omega-3 provide a protection? *PloS One*, 11(2): e0149191.

BADAMJAV R, SONOM D, WU Y, ZHANG Y, KOU J, YU B, LI F (2020) The protective effects of Thalictrum minus L. on lipopolysaccharide-induced acute lung injury. *J Ethnopharmacol*, 248: 112355.

BARRY FP, MURPHY JM (2004) Mesenchymal stem cells: clinical applications and biological characterization. *Int J Biochem Cell Biol*, 36(4): 568-584.

DE LEON JAD, BORGES CR (2020) Evaluation of oxidative stress in biological samples using the thiobarbituric acid reactive substances assay. *JoVE J Visual Exp*, 159: e61122.

DOMSCHEIT H, HEGEMAN MA, CARVALHO N, SPIETH PM (2020) Molecular dynamics of lipopolysaccharide-induced lung injury in rodents. *Front Physiol*, 11: 36.

DOS SANTOS HAUPENTHAL DP, MENDES C, DE BEM SILVEIRA G, ZACCARON RP, CORRÊA ME AB, NESI RT, SILVEIRA PCL (2020) Effects of treatment with gold nanoparticles in a model of acute pulmonary inflammation induced by lipopolysaccharide. *J Biomed Mat Res Part A*, 108(1): 103-115.

EL BANA E, SHAWKY L (2019) The appropriate time for stem cell transplantation in albino rat with amiodarone-induced lung fibrosis: histological and immunohistochemical study. *Egypt J Histol*, 42(1): 121-132.

EL-GHAZALY MA, FADEL N, RASHED E, EL-BATAL A, KENAWY SA (2017) Anti-inflammatory effect of selenium nanoparticles on the inflammation induced in irradiated rats. *Can J Physiol Pharmacol*, 95(2): 101-110.

FENG X, XU W, LI Z, SONG W, DING J, CHEN X (2019) Immunomodulatory nanosystems. *Advanced Sci*, 6(17): 1900101.

FLORES JV, KERNA NA, CHAWLA S, CARSRUD NDV, HOLETS HM, BROWN SM, OBI NJ (2022) A comprehensive review of stem cells and applications in specific diseases and regenerative therapy. *EC Clin Med Case Rep*, 5: 95-113.

GAD SS, ISMAIL SH, ABDELRAHIM DS (2021) Comparative study of the effect of sliver and selenium nanoparticles on bacterial and viral hepatic infection via modulating oxidative stress and DNA fragmentation. *J Biochem Mol Toxicol*, 36(2).

GARCÍA-GARCÍA ML, TOVILLA-ZÁRATE CA, VILLAR-SOTO M, JUÁREZ-ROJOP IE, GONZÁLEZ-CASTRO TB, GENIS-MENDOZA AD, MARTINEZ-MAGAÑA JJ (2022) Fluoxetine modulates the pro-inflammatory process of IL-6, IL-1β and TNF-α levels in individuals with depression: a systematic review and meta-analysis. *Psychiatry Res*, 307: 114317.

GEBRAAD A, OHLSBOM R, MIETTINEN JJ, EMEH P, PAKARINEN TK, MANNINEN M, MIETTINEN S (2022) Growth response and differentiation of bone marrow-derived mesenchymal stem/stromal cells in the presence of novel multiple myeloma drug melflufen. *Cells*, 11(9): 1574.

GHOLAMNEZHAD Z, SAFARIAN B, ESPARHAM A, MIRZAEIir M, ESMAEILZADEH M, BOSKABADYo MH (2022) The modulatory effects of exercise on lipopolysaccharide-induced lung inflammation and injury: A systemic review. *Life Sci*, 293: 120306.

HU Q, ZHANG Y, LOU H, OU Z, LIU J, DUAN W, JU Z (2021) GPX4 and vitamin E cooperatively protect hematopoietic stem and progenitor cells from lipid peroxidation and ferroptosis. *Cell Death Dis*, 12(7): 706.

LAFERRIERE CA, PANG DS (2020) Review of intraperitoneal injection of sodium pentobarbital as a method of euthanasia in laboratory rodents. *J Am Assoc Lab Animal Sci*, 59(3): 254-263.

LIU X, GUAN PY, YU CT, YANG H, SHAN AS, FENG XJ (2022) Curcumin alleviated lipopolysaccharide-induced lung injury via regulating the Nrf2-ARE and NF-κB signaling pathways in ducks. *J Sci Food Agriculture*, 102(14): 6603-6611.

LOWRY O, ROSEBROUGH N, FARR AL, RANDALL R (1951) Protein measurement with the Folin phenol reagent. *J Biol Chem*, 193(1): 265-275.

LU F, WANG F, CHEN Z, HUANG H (2017) Effect of mesenchymal stem cells on small intestinal injury in a rat model of acute necrotizing pancreatitis. *Stem Cell Res Therapy*, 8(1): 1-13.

MALTAIB Z, EMANSY A, ELMAHLAWY AM, SABRY D (2017) The possible ameliorative effect of mesenchymal stem cells and curcumin on bleomycin-induced lung injuries in the adult male rats: histological and immunohistochemical study. *J Stem Cell Res Therapy,* 7(389): 2.

MOKHBER DEZFOULI MR, JABBARI FAKHR M, SADEGHIAN CHALESHTORI S, DEHGHAN MM, VAJHI A, MOKHTARI R (2018) Intrapulmonary autologous transplant of bone marrow-derived mesenchymal stromal cells improves lipopolysaccharide-induced acute respiratory distress syndrome in rabbit. *Critical Care*, 22(1): 1-13.

MOKHTARI-ZAER A, NOROUZI F, ASKARI VR, KHAZDAIR MR, ROSHAN NM, BOSKABADY M, BOSKABADY MH (2020) The protective effect of Nigella sativa extract on lung inflammation and oxidative stress induced by lipopolysaccharide in rats. *J Ethnopharmacol*, 253: 112653.

NI S, WANG D, QIU X, PANG L, SONG Z, GUO K (2015) Bone marrow mesenchymal stem cells protect against bleomycin-induced pulmonary fibrosis in rats by activating Nrf2 signaling. *Int J Clin Exp Pathol,* 8(7): 7752.

PENG F, YIN H, DU B, NIU K, YANG Y, WANG S (2022) Anti-inflammatory effect of flavonoids from chestnut flowers in lipopolysaccharide-stimulated RAW 264.7 macrophages and acute lung injury in mice. *J Ethnopharmacol*, 290: 115086.

RAAFAT MH, HAMAM GG, FARHAN MS, SABBAGH LM, ABEDULDAEM NM, SHARAF AM (2018) Evaluation of the possible therapeutic role of omega-3 on ankle joint and lung in a model of rheumatoid arthritis in rats: A histological and immunohistochemical study. *Egypt J Histol,* 41(3): 250-263.

SENTKOWSKA A, PYRZYŃSKA K (2022) The influence of synthesis conditions on the antioxidant activity of selenium nanoparticles. *Molecules,* 27(8): 2486.

SHA J, ZHANG H, ZHAO Y, FENG X, HU X, WANG C, FAN H (2019) Dexmedetomidine attenuates lipopolysaccharide-induced liver oxidative stress and cell apoptosis in rats by increasing GSK-3β/MKP-1/Nrf2 pathway activity via the α2 adrenergic receptor. *Toxicol Applied Pharmacol,* 364: 144-152.

SHAHABI R, ANISSIAN A, JAVADMOOSAVI SA, NASIRINEZHAD F (2021) Protective and anti-inflammatory effect of selenium nanoparticles against bleomycin-induced pulmonary injury in male rats. *Drug Chem Toxicol,* 44(1): 92-100.

SHALABY SM, AMAL S, ABD-ALLAH SH, SELIM AO, SELIM SA, GOUDA ZA, ABDELAZIM S (2014) Mesenchymal stromal cell injection protects against oxidative stress in Escherichia coli–induced acute lung injury in mice. *Cytotherapy,* 16(6): 764-775.

SOLIMAN MG, MANSOUR HA, HASSAN WA, EL-SAYED RA, HASSAAN NA (2018) Mesenchymal stem cells therapeutic potential alleviate lipopolysaccharide- induced acute lung injury in rat model. *J Biochem Mol Toxicol,* 32(11): e22217.

SONG D, CHENG Y, LI X, WANG F, LU Z, XIAO X, WANG Y (2017) Biogenic nanoselenium particles effectively attenuate oxidative stress-induced intestinal epithelial barrier injury by activating the Nrf2 antioxidant pathway. *ACS Applied Materials Interfaces,* 9(17): 14724-14740.

SUN R, ZHAO N, WANG Y, SU Y, ZHANG J, WANG Y, XIE K (2021) High concentration of hydrogen gas alleviates Lipopolysaccharide-induced lung injury via activating Nrf2 signaling pathway in mice. *Int Immunopharmacol,* 101: 108198.

TIAN Z, WU E, YOU J, MA G, JIANG S, LIU Y, ZHENG X (2022) Dynamic alterations in the lung microbiota in a rat model of lipopolysaccharide-induced acute lung injury. *Sci Rep,* 12(1): 4791.

VIJAYAKUMAR S, CHEN J, DIVYA M, DURÁN-LARA EF, PRASANNAKUMAR M, VASEEHARAN B (2022) A review on biogenic synthesis of selenium nanoparticles and its biological applications. *J Inorganic Organometallic Polymers Materials,* 1-16.

WANG S, WANG C, ZHANG W, FAN W, LIU F, LIU Y (2022) Bioactive nano-selenium antagonizes cobalt nanoparticle-mediated oxidative stress via the Keap1-Nrf2-ARE signaling pathway. *J Nanopart Res,* 24: 1-12.

WU H, TANG N (2021) Stem cells in pulmonary alveolar regeneration. *Development,* 148(2): dev193458.

WU SH, YU JH, LIAO YT, LIU KH, CHIANG ER, CHANG MC, WANG JP (2022) Comparison of the infant and adult adipose-derived mesenchymal stem cells in proliferation, senescence, anti-oxidative ability and differentiation potential. *Tissue Engineer Regen Med,* 19(3): 589-601.

WU X, KONG Q, XIA Z, ZHAN L, DUAN W, SONG X (2019) Penehyclidine hydrochloride alleviates lipopolysaccharide-induced acute lung injury in rats: Potential role of caveolin-1 expression upregulation. *Int J Mol Med,* 43(5): 2064-2074.

YANG H, LV H, LI H, CI X, PENG L (2019) Oridonin protects LPS-induced acute lung injury by modulating Nrf2-mediated oxidative stress and Nrf2-independent NLRP3 and NF- κB pathways. *Cell Commun Signal,* 17(1): 1-15.

YE S, YANG X, WANG Q, CHEN Q, MA Y (2020) Penehyclidine hydrochloride alleviates lipopolysaccharide-induced acute lung injury by ameliorating apoptosis and endoplasmic reticulum stress. *J Surg Res,* 245: 344-353.

ZAAFAN M A, ZAKI HF, EL-BRAIRY AI, KENAWY SA (2016) Pyrrolidine dithiocarbamate attenuates bleomycin-induced pulmonary fibrosis in rats: Modulation of oxidative stress, fibrosis, and inflammatory parameters. *Exp Lung Res,* 42(8-10): 408-416.

ZAKARIA DM, ZAHRAN NM, ARAFA SAA, MEHANNA RA, ABDEL-MONEIM RA (2021) Histological and physiological studies of the effect of bone marrow-derived mesenchymal stem cells on bleomycin-induced lung fibrosis in adult albino rats. *Tissue Engineer Regener Med,* 18: 127-141.

ZHANG J, JIAO K, LIU J, XIA Y (2018) Metformin reverses the resistance mechanism of lung adenocarcinoma cells that knocks down the Nrf2 gene. *Oncology Lett,* 16(5): 6071-6080.

ZHANG S, SHI B (2017) Erythropoietin modification enhances the protection of mesenchymal stem cells on diabetic rat-derived Schwann cells: implications for diabetic neuropathy. *BioMed Res Int,* 2017.

ZHANG W, ZHANG F, SHI H, TAN R, HAN S, YE G, LIU X (2014) Comparisons of rabbit bone marrow mesenchymal stem cell isolation and culture methods in vitro. *PLoS One,* 9(2): e88794.